Single ionization of helium by 1-MeV protons

A. B. Voitkiv
Heinrich-Heine-Universität Düsseldorf, Universitätsstrasse 1, 40225 Düsseldorf, Germany
(Received 4 January 2017; revised manuscript received 3 February 2017; published 31 March 2017)

We consider the basic collision dynamics of single ionization of helium by 1-MeV protons using distorted-wave models and the first Born approximation. A good agreement is found between results of the distorted-wave models and recent experimental data [H. Gassert, O. Chuluunbaatar, M. Waitz *et al.*, Phys. Rev. Lett. **116**, 073201 (2016)] for electron emission into the azimuthal plane. However, unexpected discrepancies are observed between the theoretical results and the experimental data for the emission into the collision plane. Our consideration also shows that even though these collisions belong to the regime of weak perturbations, substantial differences exist between the results of the distorted-wave models and the first Born approximation.

DOI: 10.1103/PhysRevA.95.032708

I. INTRODUCTION

The studies of helium ionization by fast ions enable one to explore many interesting features of the dynamical behavior of few-body quantum systems. During the last 15 years the exploration of the basic dynamics of single ionization of helium by fast charged projectiles has been one of the hot topics in the field of ion-atom collisions [1–12].

In a well-known experiment [2] (see also [1]) the fully differential cross section (FDCS) for single ionization of helium by 100-MeV/u C^{6+} projectiles was measured. Although the projectile was a multiply charged ion ($Z_p = 6$ a.u.), the collision velocity v was so high ($v \approx 58$ a.u.) that the parameter $\eta_p = Z_p/v$, which characterizes the effective strength of the projectile-target interaction, was merely ≈ 0.1 suggesting that even the simplest theoretical approach—the first Born approximation (FBA)—should yield a reasonably good description of this process.

Indeed, a good agreement between experiment and the first Born theory was observed [1,2] for electron emission into the so-called collision plane which is spanned by the vectors of the initial and final projectile momenta (and in which the emission is normally maximal). However, large discrepancies were found for electron emissions outside this plane.

According to the FBA, the interaction between the projectile and the target nucleus does not contribute to the transition amplitude (see, e.g., [13]). It was therefore suggested in [2] that the disagreement between experiment and theory arises from the influence of this interaction on the collision dynamics.

A number of theoretical approaches, including the second Born, the Glauber, the continuum-distorted-wave eikonal-initial-state, and the symmetric-eikonal approximations, were applied to calculate the fully differential cross sections for ionization in collisions with fast bare ions [1,3–8,11]. These approaches, which are superior to the first Born approximation, predict a nonzero contribution to the transition amplitude from the interaction between the projectile and the target core (the target nucleus + the "passive" target electron).

All these approaches, as well as recent coupled-channel calculations [14], yield quite close results [3] for ionization by 100-MeV/u C^{6+} projectiles. All of them predicted noticeable deviations in the electron emission pattern outside the scattering plane from the FBA results. They, however, did not lead to any better overall agreement with the experiment but instead made it even worse. For instance, for electron emission into the plane, perpendicular to the transverse momentum transfer, all of them predicted a minimum exactly where—according to the experiment—a maximum should be [15].

The role of experimental uncertainties in helium ionization by 100-MeV/u C^{6+}, which are caused by a nonzero temperature of the target gas and a finite size of the projectile beam, was studied in [10] where it was concluded they are not sufficient for a full explanation of the disagreement between theory and experiment.

The effect of the non-Coulomb part of the interaction between the projectile and the target core, as a possible reason for the disagreement, was studied in [11]. However, it was found there that the deviation of the projectile–target-core interaction from the purely Coulomb one affects the cross sections only at relatively large transverse momentum transfers and, therefore, cannot be the reason for the disagreement.

More recently, the possible role of the coherence properties of the projectile beam in ionization was discussed in a number of articles (see, e.g., [16,17] and references therein). The lack (or a low degree) of coherence in an experimentally prepared beam could, according to [16,17], be responsible for the observed discrepancies between experimental results and the "conventional" theory of ion-atom collisions (which describes free particles by plane waves with well-defined momenta). A seemingly different explanation of the differences between theory and experiment was proposed in [18] where it was related to the degree to which the incident beam was uncollimated.

The present work is motivated by a recent experiment [12] that explored the basic dynamics of single ionization of helium by 1-MeV protons. The authors used an experimental setup which enabled them to reach the highest resolution ever reported for ionizing ion-atom collisions. Their experimental results were compared with FBA calculations [12] and no large qualitative disagreement between experiment and theory, which would be similar to that observed for ionization by 100-MeV/u C^{6+}, was found.

The main goal of the present article is to explore, while remaining within the conventional theory of ion-atom collisions, how accurately one can reproduce the experimental data of [12] by using theoretical approaches which are more sophisticated than the first Born approximation. Taking into account that the collisions with 1-MeV protons are in the regime of fast

collisions at (relatively) weak perturbations ($\eta_p = Z_p/v \approx 0.16 \ll 1$) one can expect that distorted-wave models represent a good tool for describing the ionization process. Atomic units are used throughout except where otherwise stated.

II. THEORETICAL APPROACHES

Typical values of the momentum transfer to the target in collisions resulting in ionization of helium do not exceed a few atomic units. Besides, in the target reference frame the overwhelming majority of the emitted electrons have energies not exceeding a few tens of electronvolts. Therefore, by considering the momentum balance in the collision it is not difficult to conclude that the change in the momentum of the target nucleus caused by the collision also does not exceed a few atomic units. Consequently, the recoil velocity $u_{\rm rec}$ of the target nucleus in the collision is of the order of 10^{-4} a.u.

In experiments aimed at the exploration of the basic collision dynamics the target is cooled down to very low temperatures. For instance, in the experiment of [12] the helium target was cooled to $\lesssim$1 K that corresponds to atomic velocities u_0 of the order of 10^{-5} a.u. such that the target atoms may be considered as being initially at rest with respect to each other. Besides, despite the recoil velocity of the target nucleus $u_{\rm rec} \sim 10^{-4}$ a.u. is substantially larger than u_0 (as it should be in order to be able to experimentally explore the basic collision dynamics), it nevertheless is also negligibly small compared to the velocities of the other particles (the projectile and the electron) participating in the collision. Therefore, we shall suppose, as usual, that the target nucleus rests in the collision and take its position as the origin of our reference frame.

Further, what has been said in the first paragraph of this section about the momentum balance also implies that the change in the momentum of the heavy projectile in the collision is negligible compared to its initial value. This enables us to start our consideration with the semiclassical approximation in which the projectile is supposed to move along a straight-line classical trajectory $\mathbf{R}_p(t) = \mathbf{b} + \mathbf{v}t$, where $\mathbf{b}$ is the impact parameter, $\mathbf{v}$ is the projectile (collision) velocity, and t is the time.

It is worth noting that the approximations made assuming that in the collision the target nucleus remains at rest and the projectile moves along a straight line by no means imply that the energy and momentum balance in the collision (and, in particular, the important role of the target nucleus in the momentum balance) will not be properly described. In fact these approximations simply mean that the corrections of the order of $m_e/M \sim 10^{-3}$–10^{-4}, where m_e is the electron mass and M is the mass of the target nucleus (or the projectile), will be ignored in the energy-momentum balance and the transition amplitude. This is quite obvious from simple physical estimates, which were given in the previous paragraphs of this section, and can also be shown in a formal way using, for instance, the results of [19] given on pp. 133–134 of their paper (see also [20], pp. 290–294).

In the semiclassical approximation the corresponding Schrödinger equation reads

$$i\frac{\partial}{\partial t}\Psi = \hat{H}\Psi, \tag{1}$$

where the semiclassical Hamiltonian $\hat{H}$, which explicitly depends on time, is given by

$$\hat{H} = \hat{H}_a - \frac{Z_p}{|\mathbf{r}_1 - \mathbf{R}_p|} - \frac{Z_p}{|\mathbf{r}_2 - \mathbf{R}_p|} + \frac{2\,Z_p}{R_p}. \tag{2}$$

Here, $\hat{H}_a$ is the Hamiltonian for a free helium,

$$\hat{H}_a = \frac{\hat{\mathbf{p}}_1^2}{2} - \frac{2}{r_1} + \frac{\hat{\mathbf{p}}_2^2}{2} - \frac{2}{r_2} + \frac{1}{r_{12}}, \tag{3}$$

where $\mathbf{r}_j$ and $\hat{\mathbf{p}}_j$ ($j = 1,2$) are the electron coordinates and momentum operators, respectively, and $r_{12} = |\mathbf{r_1} - \mathbf{r_2}|$. The last three terms in Eq. (2) describe the interaction of the atomic electrons and the nucleus with the projectile.

It is customary (see, e.g., [21,22]) to split the electron-electron interaction according to

$$\frac{1}{r_{12}} = \sum_{j=1}^{2} w_j(r_j) + W, \tag{4}$$

where $w_j(r_j)$ ($j = 1,2$) are one-electron operators and W is a nonseparable part of the electron-electron interaction. The terms $w_j(r_j)$ can be combined in Eq. (3) with the interactions $-2/r_j$ to form an average (mean-field) interaction acting on the electrons and W represents a correlation potential.

It is well known that electron-electron correlations play a crucial role in double ionization of helium by single photons and very fast low-charged nuclei. These correlations can also be of paramount importance for single ionization of helium provided it involves excitation and decay of autoionizing states. To our knowledge, however, there is no evidence that electron-electron correlations have a significant impact on single ionization of helium in collisions with fast bare ions when electron emission energy is far from those values which can be populated via autoionization. The minimum emission energy, for which autoionizing states could unveil themselves, lies above 30 eV which is very far from the range of emission energies ($\leqslant$10 eV) discussed in [12].

Keeping this in mind and following our previous considerations of single ionization of helium by fast bare nuclei [7,8,11], we shall neglect the correlation interaction $\hat{W}$ and regard ionizing collisions as an effectively three-body process which involves the projectile, the "active" electron of the helium target, and the "frozen" target core. The latter consists of the target nucleus and the "passive" electron, is assumed to be rigid in the collision, and produces a field which acts on the active electron in the initial and final collision channels. The same field acts also on the projectile in the collision.

The field produced by the target core is approximated using the potential

$$u(\xi) = \frac{1}{\xi} + (1 + \beta\xi)\frac{\exp(-\alpha\xi)}{\xi},$$

where $\boldsymbol{\xi}$ ($|\boldsymbol{\xi}| = \xi$) denotes either the coordinate $\mathbf{r}$ of the active target electron or the coordinate $\mathbf{R}_p$ of the projectile. Following [22] we set $\alpha = 3.36$ and $\beta = 1.665$. With this choice $\phi(\mathbf{r})$ almost coincides with the exact Hartree-Fock potential.

Thus, our treatment of single ionization of helium by fast projectiles is based on the following effective single-electron

Schrödinger equation:

$$i\frac{\partial}{\partial t}\psi(\mathbf{r},t) = \hat{H}_{\rm eff}\,\psi(\mathbf{r},t), \tag{5}$$

with

$$\hat{H}_{\rm eff} = \hat{H}_0 - \frac{Z_p}{|\mathbf{r}-\mathbf{R}_p|} + Z_p\,u(R_p), \tag{6}$$

where

$$\hat{H}_0 = \frac{\hat{\mathbf{p}}^2}{2} - u(r) \tag{7}$$

is the Hamiltonian for the free atom, and $\mathbf{r}$ and $\hat{\mathbf{p}}$ are the coordinates and the momentum operator, respectively, of the active electron. The fact that helium has two electrons will be taken into account by multiplying the obtained single-electron cross sections by a factor of 2.

The post and prior forms of the semiclassical transition amplitude $a_{\rm fi}(\mathbf{b})$ are given by

$$a_{\rm fi}^{\rm post}(\mathbf{b}) = -i\int_{-\infty}^{+\infty} dt\left\langle\left(\hat{H}_{\rm eff} - i\frac{\partial}{\partial t}\right)\chi_f(t)\middle|\psi^{(+)}(t)\right\rangle \tag{8}$$

and

$$a_{\rm fi}^{\rm prior}(\mathbf{b}) = -i\int_{-\infty}^{+\infty} dt\left\langle\psi^{(-)}(t)\middle|\left(\hat{H}_{\rm eff} - i\frac{\partial}{\partial t}\right)\phi_i(t)\right\rangle, \tag{9}$$

respectively. Here $\psi^{(-)}$ ($\psi^{(+)}$) is the solution of the Schrödinger equation (5) with the "in" ("out") boundary conditions, and $\phi_i(t)$ ($\chi_f(t)$) is the initial (final) state of the electron.

A. FBA

In the first-order (or first Born) approximation ϕ_i and $\psi^{(-)}$ (or $\psi^{(+)}$ and χ_f, respectively) are approximated by

$$\begin{aligned}\phi_i &= \xi_0\,\exp(-i\varepsilon_0 t),\\ \psi^{(-)} &= \xi_{\mathbf{p}}\,\exp(-i\varepsilon_{\mathbf{p}} t),\end{aligned} \tag{10}$$

where ξ_0 and $\xi_{\mathbf{p}}$ are eigenstates of the Hamiltonian (7), ξ_0 is the initial (ground) state of the electron in the free atom, and $\xi_{\mathbf{p}}$ describes the emitted electron moving in the field of the atom with an asymptotic momentum $\mathbf{p}$. These states as well as the energy ε_0 of the electron initial state are obtained by a (numerical) solution of the stationary Schrödinger equation with the Hamiltonian (7).

According to Eqs. (8)–(10) the interaction, which couples the initial and final states [Eq. (10)] in the FBA transition amplitude, is given by $\hat{H}_{\rm eff} - \hat{H}_0 = -\frac{Z_p}{|\mathbf{r}-\mathbf{R}_p|} + Z_p\,u(R_p)$, thus it is the "physical" interaction between the projectile and the target. One of the peculiarities of the FBA is that, since the initial and final internal states of the target are orthogonal, the interaction between the projectile and the target nucleus (the target core) simply drops out from the transition amplitude thus having no effect on the calculated cross sections.

B. Distorted-wave models

The ionization process will also be considered by applying two distorted-wave approaches: the continuum-distorted-wave eikonal-initial-state (CDW-EIS) and the symmetric eikonal (SEA) models. The former was proposed in [23] for considering ionization, the latter was initially suggested in [24] for describing electron capture.

In the distorted-wave models ϕ_i and $\psi^{(-)}$ (or $\psi^{(+)}$ and χ_f) are approximated by

$$\begin{aligned}\phi_i &= L_i\,\xi_0\,\exp(-i\varepsilon_0 t),\\ \psi^{(-)} &= L_f\,\xi_{\mathbf{p}}\exp(-i\varepsilon_{\mathbf{p}} t),\end{aligned} \tag{11}$$

where L_i and L_f are the so-called distortion factors for the initial and final atomic states, respectively, which (approximately) describe the distortion of these states caused by the interaction with the projectile.

Unlike the FBA approximation, in distorted-wave models the post and prior forms of the transition amplitude in general do not coincide. Besides, since in these models the projectile-target interaction is already partly included in the states (11) the residual interaction, which causes the transitions, differs from the physical one of the FBA.

CDW-EIS. In the CDW-EIS model these factors are chosen according to

$$\begin{aligned}L_i = L_i^{\rm eik} &= \exp\left(-iZ_p\int_{-\infty}^{t} dt' u(R_p(t'))\right)\\ &\quad\times\exp\left(iZ_p\int_{-\infty}^{t} dt' 1/s(t')\right)\\ L_f = L^{\rm cdw} &= \exp\left(-iZ_p\int_{+\infty}^{t} dt' u(R_p(t'))\right)\\ &\quad\times\exp[(\pi Z_p/(2\kappa)]\Gamma(1+iZ_p/\kappa)\\ &\quad\times{}_1F_1(-iZ_p/\kappa;1;-i\,\kappa\,s - i\,\boldsymbol{\kappa}\cdot\mathbf{s}),\end{aligned} \tag{12}$$

where $\mathbf{s} = \mathbf{r} - \mathbf{R}_p$, $\boldsymbol{\kappa} = \mathbf{p} - \mathbf{v}$ is the relative velocity of the emitted electron with respect to the projectile, Γ is the gamma function, and ${}_1F_1$ is the confluent hypergeometric function (see, e.g., [25]).

SEA. In the SEA model the distortion factors are taken as

$$\begin{aligned}L_i = L_i^{\rm eik} &= \exp\left(-iZ_p\int_{-\infty}^{t} dt' u(R_p(t'))\right)\\ &\quad\times\exp\left(iZ_p\int_{-\infty}^{t} dt' 1/s(t')\right),\\ L_f = L_f^{\rm eik} &= \exp\left(-iZ_p\int_{+\infty}^{t} dt' u(R_p(t'))\right)\\ &\quad\times\exp\left(iZ_p\int_{+\infty}^{t} dt' 1/s(t')\right).\end{aligned} \tag{13}$$

Comparing Eqs. (13) with Eqs. (12) we see that in both models the distortion factor for the initial state is the same. However, the full Coulomb distortion factor in the final state of the CDW-EIS is replaced in the SEA by its asymptotic (eikonal) form (in which also the relative velocity $\boldsymbol{\kappa}$ of the emitted electron is approximated by $-\mathbf{v}$).

The semiclassical transition amplitude depends on the impact parameter which is not an observable quantity. Therefore the basic quantum dynamics of the collision cannot be treated with such an amplitude. However, for collisions with small projectile scattering angles and negligible recoil velocities of the target nucleus, the quantum transition amplitude $S_{\rm fi}$ can

be obtained from the semiclassical one according to (see, e.g., [7])

$$S_{\rm fi}(\mathbf{Q}) = \frac{1}{2\pi}\int d^2\mathbf{b}\,\exp(i\mathbf{Q}\cdot\mathbf{b})\,a_{\rm fi}(\mathbf{b}). \tag{14}$$

Here, $\mathbf{Q}$ is the two-dimensional part of the momentum transfer $\mathbf{q}$ to the target, which is perpendicular to the projectile velocity, $\mathbf{Q}\cdot v = 0$. The total momentum transfer is given by

$$\mathbf{q} = (\mathbf{Q}, q_{\rm min}), \tag{15}$$

where $q_{\rm min} = (\varepsilon_f - \varepsilon_i)/v$ is the minimum momentum transfer and ε_i and ε_f are the initial and final energies of the electron.

Since the semiclassical transition amplitude and the amplitude of Eq. (14) are related to each other by the Fourier transformation the following identity holds (Parseval's theorem):

$$\int d^2\mathbf{Q}\,|S_{\rm fi}(\mathbf{Q})|^2 = \int d^2\mathbf{b}\,|a_{\rm fi}(\mathbf{b})|^2. \tag{16}$$

The CDW-EIS and SEA models have been successfully used for calculating such quantities as the total cross sections and energy-angular distributions of the emitted electrons. As it follows from Eq. (16) these quantities can be obtained either by integrating the absolute square of the amplitude [Eq. (14)] over the transverse momentum transfer or the absolute square of the semiclassical transition amplitude over the impact parameter.

The factors L_i and L_f in Eqs. (12) and (13) include also the distortion due to the interaction between the projectile and the target nucleus (target core). However, this distortion appears there just as a phase factor which is independent of the electron coordinates. Therefore, after squaring the semiclassical transition amplitude $a_{\rm fi}(\mathbf{b})$ the result already does not depend on the interaction between the heavy particles. Consequently this interaction does not influence cross sections which are obtained by integrating over the impact parameter (or the transverse momentum transfer). As a result, this interaction can simply be omitted in the Hamiltonian (6) and the distortion factors (12)–(13) when such cross sections are calculated, which greatly simplifies the computation.

The underlying physical reason for this is that in fast ion-atom collisions the interaction between the projectile and the target core practically does not change the motion of these heavy particles in the reaction zone. As a result, any indirect coupling between the electron and the heavy particles, which would be caused by the interaction between the latter ones, is practically absent.

This interaction, however, becomes of great importance when cross sections differential in the projectile scattering angle (or in the transverse momentum transfer in the collision) are studied (see, e.g., [26,27]). Therefore, in our case it is necessary to take the interaction between the projectile and the target core into account, keeping in particular, in Eqs. (12) and (13), the phases which are related to this interaction. In order to stress this point, in what follows we shall label the CDW-EIS and the SEA models, in which the internuclear interaction is not ignored, by the CDW-EIS-NN and the SEA-NN, respectively.

The CDW-EIS-NN and SEA-NN models amount to taking into account the first-order terms of corresponding distorted-wave perturbative expansions. In fast collisions with the emission of low-energy electrons their expansion parameters are proportional to Z_p/v^2. This is to be compared with the expansion parameter of the standard Born expansion $\sim Z_p/v$. In the limit of very weak projectile-target interactions the results of the CDW-EIS-NN and SEA-NN go over into those of the FBA.

III. RESULTS AND DISCUSSION

Our numerical results, which will be reported in this section, have been obtained with computer codes developed using the post version of the CDW-EIS and the prior version of the SEA (for further details see, e.g., [27] and [7], respectively). In what follows we suppose that in the rest frame of the target nucleus (our reference frame) the projectile is incident along the z axis, $\mathbf{v} = (0,0,v)$.

A. Fully differential cross sections

The basic dynamics of single ionization of helium can be described by the FDCS, $\frac{d\sigma^{(+)}}{d^2\mathbf{Q}d^3\mathbf{p}}$, where $\mathbf{Q}$ is the transverse part of the total momentum transfer $\mathbf{q}$ to the target and $\mathbf{p} = (p,\vartheta_{\mathbf{p}},\varphi_{\mathbf{p}})$ is the momentum of the emitted electron. Following [12] we choose the x axis to be along $\mathbf{Q}$.

The total momentum transfer is given by Eq. (15) where $q_{\rm min} = (\varepsilon_p - \varepsilon_0)/v$ with $\varepsilon_0 = -24.6$ eV and ε_p being the energy of the ground state of the Hamiltonian (7) and the energy of the emitted electron, respectively.

Using the FBA, the CDW-EIS-NN, and the SEA-NN, we calculated the FDCS for several values of the electron emission energy ε_p ($1 \leqslant \varepsilon_p \leqslant 100$ eV) and the total momentum transfer q ($0.25 \leqslant q \leqslant 2$ a.u.). The main conclusion which can be drawn from these calculations is that despite $\eta_p \ll 1$ the results of the distorted-wave models substantially differ from those of the FBA. On the other hand, the differences between results of the CDW-EIS-NN and the SEA-NN models are comparatively modest and decrease, as expected, when the electron emission energy decreases, practically vanishing at low emission energies, where the velocity of the emitted electron is much smaller than the collision velocity.

In Figs. 1–4 we compare our results for the FDCS [28] with the experimental data of [12]. Theoretical results shown in Figs. 1 and 2 are the cross sections calculated at fixed values of the electron emission energy (6.5 eV) and the total momentum transfer (0.75 a.u.). In Figs. 3 and 4 the theoretical cross sections were averaged over $3 \leqslant \varepsilon_{\mathbf{p}} \leqslant 10$ eV and $0.5 \leqslant q \leqslant 1$ a.u. (which corresponds to the experimental bin sizes of [12]).

For these low emission energies the CDW-EIS-NN and the SEA-NN yield very close results (the results of the SEA-NN are therefore not shown in the figures). The results of the CDW-EIS-NN and the FBA are presented on an absolute scale.

In Figs. 1 and 3 the FDCS is given for the collision plane [the ($\mathbf{Q}$, $\mathbf{v}$) plane] and is plotted as a function of the polar emission angle $\vartheta_{\mathbf{p}}$ of the electron. In both figures the experimental data have been normalized to the theoretical results by setting the maximum of the experimental cross section to be equal to the maximum of the theoretical one obtained using the CDW-EIS-NN (we note, however, that these maxima are not located at the same emission angle).

In Figs. 2 and 4 the FDCS is given for the azimuthal plane which is perpendicular to the collision velocity ($\vartheta_{\mathbf{p}} = 90^\circ$). In

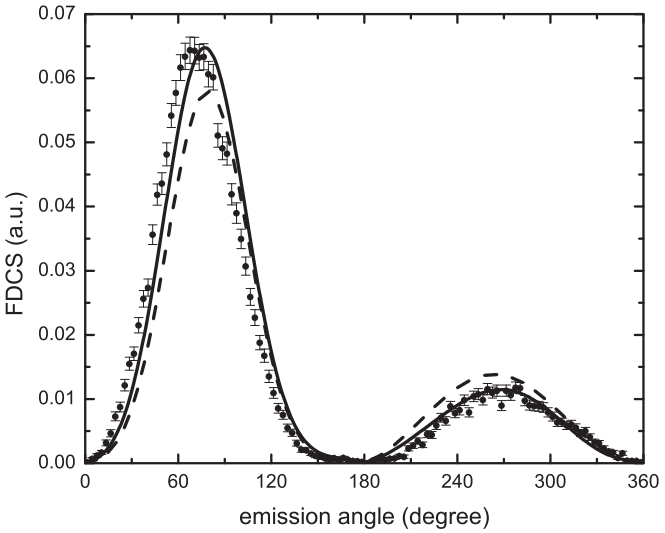

FIG. 1. FDCS for single ionization of helium by 1-MeV protons in the collision plane plotted as a function of the polar emission angle. The electron emission energy is $\varepsilon_p = 6.5$ eV and the total momentum transfer $q = 0.75$ a.u. Symbols: experimental data from [12]. Solid and dash curves are the results of the CDW-EIS-NN and the FBA, respectively.

these figures the FDCS is plotted as a function of the azimuthal emission angle $\varphi_{\mathbf{p}}$ of the electron. Because of the symmetry with respect to the vector $\mathbf{Q}$, which the FDCS possesses in the azimuthal plane, it is sufficient to consider the range $0^\circ \leqslant \varphi_{\mathbf{p}} \leqslant 180^\circ$. The following main conclusions can be drawn from the figures.

First, in both planes the CDW-EIS-NN yields substantially better agreement with the experimental data than the FBA. Second, in the collision plane the familiar structures in the emission pattern—the so-called binary and recoil peaks—are clearly seen both in the experimental data and the theoretical

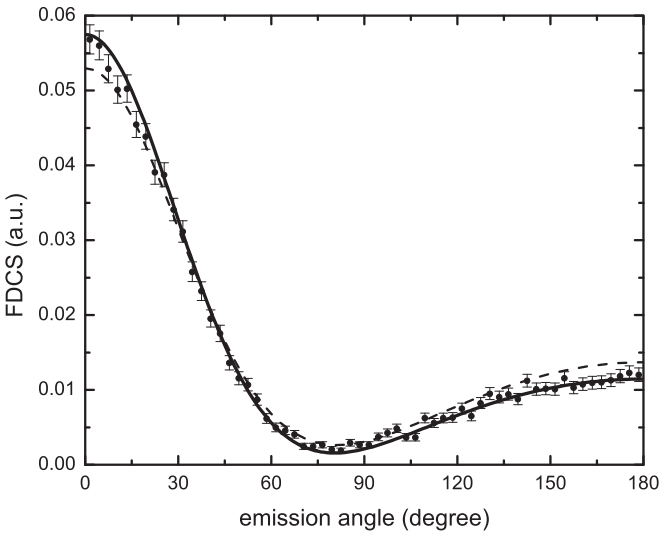

FIG. 2. Same as in Fig. 1 but for electron emission into the azimuthal plane ($\vartheta_p = 90^\circ$) given as a function of the azimuthal emission angle $\varphi_{\mathbf{p}}$.

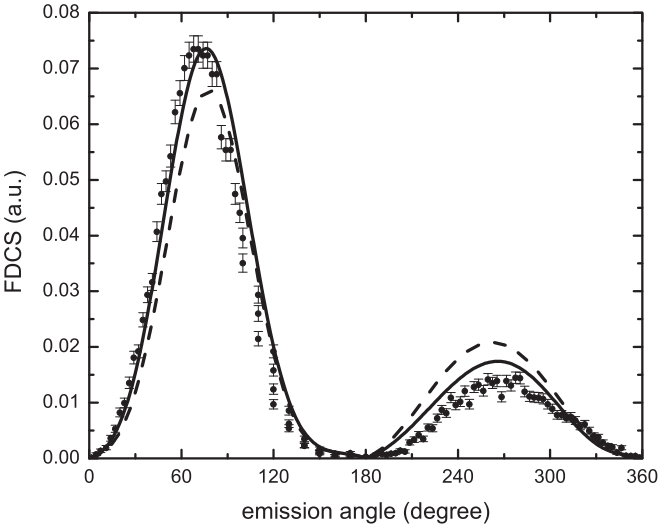

FIG. 3. Same as in Fig. 1 but averaged over the interval of the emission energies 3–10 eV and the momentum transfer 0.5–1 a.u.

results. However, the shapes of the experimental and calculated spectra are not the same. In particular, compared to the maximum in the experimental data the maximum in the calculated binary peak is shifted by about 5°–6° (7.5°–8.5° without the averaging) toward larger $\vartheta_{\mathbf{p}}$ and this shift holds almost for the whole binary peak. After the averaging the theory also overestimates the recoil-to-binary-peak ratio by about 25%. Besides, a close inspection of the recoil peak shows that there is a shift of about 5°–10° between the theoretical and experimental data but now toward smaller $\vartheta_{\mathbf{p}}$.

Third, in the azimuthal plane there is a good agreement between the CDW-EIS-NN and the experiment except for the range of large angles ($\varphi_{\mathbf{p}} \gtrsim 135^\circ$) where the theory predicts a stronger increase of the cross section with increasing $\varphi_{\mathbf{p}}$.

Compared to the results which are calculated for fixed values of the emission energy ($\varepsilon_p = 6.5$ eV) and the momentum transfer ($q = 0.75$ a.u.), the theoretical data obtained by

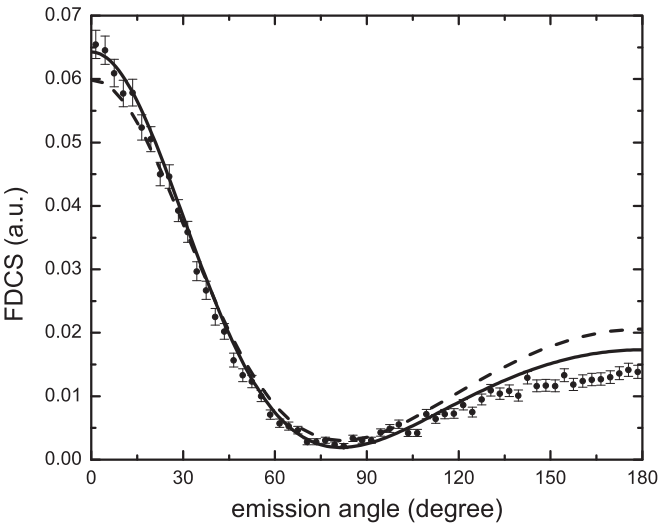

FIG. 4. Same as in Fig. 2 but averaged over the interval of emission energies 3–10 eV and the momentum transfer 0.5–1 a.u..

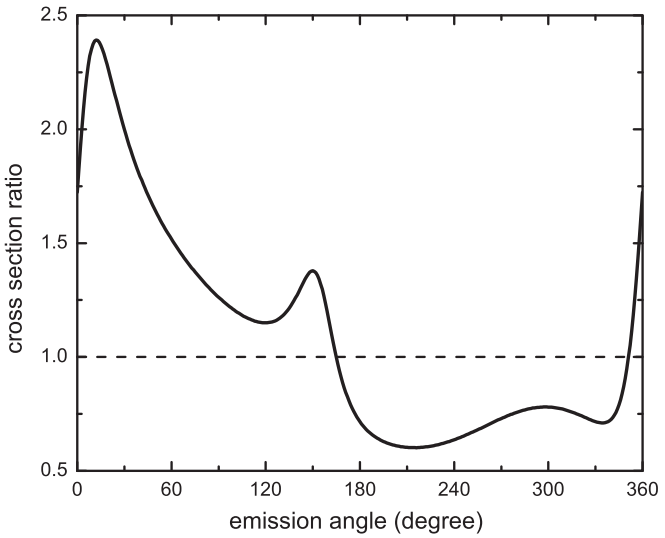

FIG. 5. Proton-to-antiproton cross section ratio given as function of the electron emission angle in the collision plane. The electron emission energy is $\varepsilon_p = 6.5$ eV and the total momentum transfer is $q = 0.75$ a.u. The solid curve and dash line are the results of the CDW-EIS-NN and the FBA, respectively.

averaging over $\varepsilon_p = 6.5 \pm 3.5$ eV and $q = 0.75 \pm 0.25$ a.u. mainly differ in that the recoil-to-binary-peak ratio somewhat increases and the position of the binary peak is slightly shifted to smaller emission angles.

The discrepancy between the positions of the experimental and calculated binary peaks is rather unexpected because even for helium ionization by 100-MeV/u C^{6+} there was a good agreement between them. Moreover, the character of this discrepancy does not suggest that the coherence properties of the projectile beam might be responsible for them.

It was already mentioned that there are substantial differences between the results of the CDW-EIS-NN and the FBA. In order to emphasize them, in Figs. 5 and 6 we show the ratio of

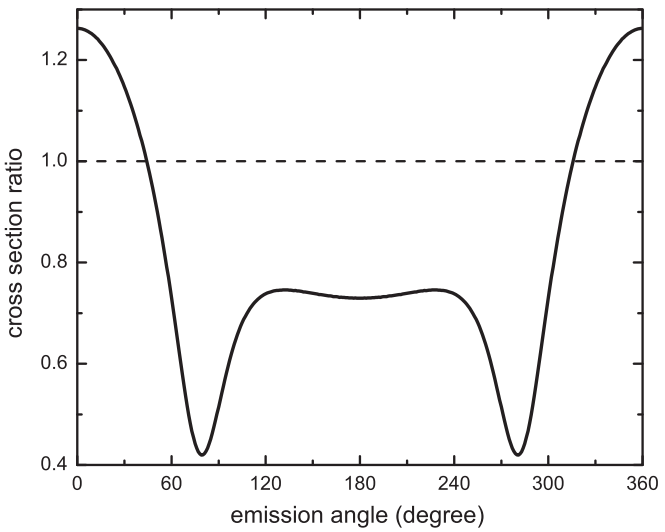

FIG. 6. Same as in Fig. 5 but for electron emission into the azimuthal plane given as a function of $\varphi_{\mathbf{p}}$.

the FDCSs in collisions with 1-MeV protons and antiprotons calculated using the CDW-EIS-NN. This ratio is given in the collision (Fig. 5) and azimuthal (Fig. 6) planes for electron emission energy of 6.5 eV and the total momentum transfer of 0.75 a.u.

It is seen in the figures that the CDW-EIS-NN predicts a strong dependence on the sign of the projectile's charge whereas according to the FBA this ratio is always equal to 1. One should note that in the case under consideration the main origin of the differences between the results of the distorted-wave models and the first Born approximation is caused by the interaction between the projectile and the target nucleus (the target core). In the first Born approximation this interaction does not contribute to the transition amplitude but, according to the distorted-wave models, has an important impact on the fully differential cross section.

B. Longitudinal momentum spectrum

It is worth mentioning that single ionization of helium by 1-MeV protons and 945-keV antiprotons was studied in [29] where the longitudinal momentum spectrum of the emitted electrons was measured and substantial differences between proton and antiproton impacts had not been observed.

However, according to our CDW-EIS calculations the proton-to-antiproton ratio of the longitudinal spectra varies between 0.7 and 1.3 in the interval $-1 \leqslant p_{\mathrm{lg}} \leqslant 1$ and between 0.65 and 1.5 for $-2 \leqslant p_{\mathrm{lg}} \leqslant 2$, where $p_{\mathrm{lg}} = \mathbf{p} \cdot \mathbf{v}/v$ is the longitudinal component of the momentum $\mathbf{p}$ of the emitted electron. The predicted dependence on the sign of the projectile charge for this spectrum is not weak and the fact that it was not seen in the experimental data of [29] could perhaps be attributed to low statistics in collisions with antiprotons that resulted in relatively large error bars. Besides, just the interval $-1 \leqslant p_{\mathrm{lg}} \leqslant 1$ was considered in [29].

C. Energy spectrum and the total cross section

We have also performed calculations for the energy spectrum of electrons emitted in single ionization of helium by 1-MeV protons and for the total cross section of this process. In contract to the case with the longitudinal momentum spectrum, where the interaction between the projectile and the emitted electron (so-called postcollision interaction, which is absent in the FBA) plays an important role, there is a little difference between the energy spectra calculated using the FBA and the distorted-wave models. Naturally, the same holds true also for the calculated total cross section. In particular, we obtained for the total cross section of helium single ionization by 1-MeV protons $\approx 2 \times 10^{-17}$ cm^2.

It is important to note that the total cross sections for single ionization of helium in fast collisions with relatively low charged nuclei ($Z_p \ll v$) calculated by treating this process as an effectively three-body problem [and using the Hamiltonian (7) to describe the free atomic states] are in very good agreement with results of the well-known Bethe-Born formula (see, e.g., [30]), which is quite accurate in this range of collision parameters. Moreover, the three-body models yield an excellent agreement with experiment for the shape of the energy spectrum of the emitted electrons (see, e.g., [7]).

IV. CONCLUSIONS

In conclusion, using the first Born approximation and two distorted-wave models—CDW-EIS-NN and SEA-NN—we have considered single ionization of helium by 1-MeV protons and compared our results with the data of the recent experiment [12]. A good agreement is found between the experimental data and our distorted-wave calculations for the most of the azimuthal plane. However, unexpected (although not very large) discrepancies between the experiment and theory are observed for the collision plane.

For 1-MeV protons the parameter $\eta_p = Z_p/v$ is much smaller than 1 and, correspondingly, the collisions under consideration belong to the regime of weak perturbations. Nevertheless, our distorted-wave calculations for the fully differential cross section and the longitudinal momentum spectrum of the emitted electrons predict substantial deviations from the results of the first Born approximation. In particular, large differences in the shape of the emission pattern are expected for helium ionization by 1-MeV protons and antiprotons.

Taking into account the differences between theory and experiment in the collision plane and a strong dependence of the emission pattern on the charge of the projectile, which is predicted by the distorted-wave models, it would be very desirable to undertake further research, theoretical and experimental, on the basic collision dynamics of helium ionization by fast protons and antiprotons.

ACKNOWLEDGMENT

We thank M. Schöffler for providing us with the experimental data in a tabular form.

[1] D. H. Madison, M. Schulz, S. Jones, M. Foster, R. Moshammer, and J. Ullrich, J. Phys. B **35**, 3297 (2002).
[2] M. Schulz, R. Moshammer, D. Fischer, H. Kollmus, D. H. Madison, S. Jones, and J. Ullrich, Nature **422**, 48 (2003).
[3] A. B. Voitkiv, B. Najjari, and J. Ullrich, J. Phys. B **36**, 2591 (2003).
[4] D. H. Madison, D. Fischer, M. Foster, M. Schulz, R. Moshammer, S. Jones, and J. Ullrich, Phys. Rev. Lett. **91**, 253201 (2003).
[5] D. Fischer, A. B. Voitkiv, R. Moshammer, and J. Ullrich, Phys. Rev. A **68**, 032709 (2003).
[6] M. Foster, D. H. Madison, J. L. Peacher, M. Schulz, S. Jones, D. Fischer, R. Moshammer, and J. Ullrich, J. Phys. B **37**, 1565 (2004).
[7] A. B. Voitkiv and B. Najjari, J. Phys. B **37**, 4831 (2004).
[8] A. B. Voitkiv, B. Najjari, R. Moshammer, M. Schulz, and J. Ullrich, J. Phys. B **37**, L365 (2004).
[9] J. Fiol, S. Otranto, and R. E. Olson, J. Phys. B **39**, L285 (2006).
[10] M. Dürr, B. Najjari, M. Schulz, A. Dorn, R. Moshammer, A. B. Voitkiv, and J. Ullrich, Phys. Rev. A **75**, 062708 (2007).
[11] A. B. Voitkiv and B. Najjari, Phys. Rev. A **79**, 022709 (2009).
[12] H. Gassert, O. Chuluunbaatar, M. Waitz *et al.*, Phys. Rev. Lett. **116**, 073201 (2016).
[13] M. R. C. McDowell and J. P. Coleman, *Introduction to the Theory of Ion-Atom Collisions* (North-Holland, Amsterdam, 1970).
[14] A. Kadyrov (private communication).
[15] We note that at an impact energy of 100-MeV/u the first Born approximation predicts for this plane practically a constant emission pattern.
[16] X. Wang *et al.*, J. Phys. B **45**, 211001 (2012).
[17] L. Sarkadi, I. Fabre, F. Navarrete, and R. O. Barrachina, Phys. Rev. A **93**, 032702 (2016).
[18] J. M. Feagin and L. Hargreaves, Phys. Rev. A **88**, 032705 (2013).
[19] M. Hirooka and S. Sunakawa, Prog. Theor. Phys. **52**, 131 (1974).
[20] D. S. F. Crothers and L. G. Dube, Adv. At. Mol. Opt. Phys. **30**, 287 (1992).
[21] J. H. McGuire, *Electron Correlation Dynamics in Atomic Collisions* (Cambridge University Press, New York, 1997).
[22] F. Martin and A. Salin, Phys. Rev. A **55**, 2004 (1997).
[23] D. S. F. Crothers and J. McCann, J. Phys. B **16**, 3229 (1983).
[24] J. M. Maidagan and R. D. Rivarola, J. Phys. B **17**, 2477 (1984).
[25] M. Abramowitz and I. Stegun, *Handbook of Mathematical Functions* (Dover, New York, 1964).
[26] V. D. Rodrigues, J. Phys. B **29**, 275 (1996).
[27] A. B. Voitkiv and J. Ullrich, Phys. Rev. A **67**, 062703 (2003).
[28] In order to make a comparison with the data from [12] we have multiplied the FCDS by $\sin\vartheta_{\mathbf{p}}$.
[29] Kh. Khayyat, T. Weber, R. Dörner, M. Achler *et al.*, J. Phys. B **32**, L73 (1999).
[30] M. Inokuti, Rev. Mod. Phys. **43**, 297 (1971).